JOURNAL OF MATERIALS SCIENCE 17 (1982) 2013–2026

A distributed dislocation stress analysis for crazes and plastic zones at crack tips

WEN-CHOU V. WANG, EDWARD J. KRAMER
Department of Materials Science and Engineering and the Materials Science Center, Cornell University, Ithaca, N.Y. 14853, USA

A distributed dislocation method is developed to obtain analytically the applied stress as well as the surface stress profile along narrow plastic zones at the tip of a crack in a homogeneous tensile stress field. Replacing the plastic zone by a continuous array of mathematical dislocations, the stress field solution of this mixed boundary value problem (the displacement profile of the plastic zone is fixed while the tensile stresses are zero across the crack) can be solved. A computer program based on this stress field solution has been constructed and tested using the analytical results of the Dugdale model. The method is then applied to determining the surface stress profiles of crazes and plane-stress plastic deformation zones grown from electron microprobe cracks in polystyrene and polycarbonate respectively. The necessary craze and zone surface displacement profiles are determined by quantitative analysis of transmission electron micrographs. The surface stress profiles, which show small stress concentrations at the craze or zone tip falling to an approximately constant value which is maintained to the crack tip, are compared with those previously computed using an approximate Fourier transform method involving estimation of the displacement profile in the crack. The agreement between the approximate method and the exact distributed dislocation method is satisfactory.

1. Introduction

It is an established experimental fact that the propagation of a crack in a normally ductile material is accompanied by plastic deformation in advance of the crack tip. A very crude estimate of the extent of the plastic zone can be made by saying that a point is inside the plastic zone if the elastic stress at the point has a value which is equal to or greater than the uniaxial yield stress [1]. Better estimates have been obtained from the von Mises yield criterion [1, 2] or from continuum plasticity [3]. Levy used finite element methods to locate the boundaries of the plastic zone from continuum plasticity, and his result showed good agreement with the observation of the plastic zone shape of an interior section of an Fe–3% Si steel plate by Hahn [4].

Plastic zones having the form of a narrow wedge-shaped layer have been observed in thin sheet mild steel by Dugdale [5] and in glassy polymers, such as poly(methyl methacrylate) (PMMA) and polystyrene, in the form of crazes [6–9]. Based on his observation in 1960, Dugdale [5] proposed a model of the crack and plastic zone, which permits an evaluation of the plastic energy dissipation by the methods of elastic–perfectly plastic continuum mechanics. This model, developed further by Barenblatt [10] (actually, he proposed a similar model earlier in 1959), by Bilby, Cottrell and Swinden [11], and by Goodier and Field [12], has been extensively used because it is simple and adequately describes the overall effect of crack tip yielding.

The plastic zone in a polymer material often occurs in the form of "crazes". The first model of an isolated craze (with no crack associated with the craze) was published by Knight [13]. Verheulpen-Heymans and Bauwens [14], Wilczynski, Liu and Hsaio [15] and recently Mills [16] have proposed different models for craze micromechanics. Investigation [6, 8, 9, 17] of the micromechanics of crazes at crack tips in trans-

0022–2461/82/072013–14$04.18/0 © *1982 Chapman and Hall Ltd.*

parent plastics has shown that the Dugdale plastic zone model provides a good starting point for predicting fracture toughness in such polymers. However, due to its oversimplified assumption of a constant yield stress along the deformation zone, the Dugdale model can describe the craze shape at a crack tip only qualitatively. Some authors [18, 19] moreover, have suggested that the Dugdale model cannot even do this.

Recently, a high resolution method for measuring the displacements along crazes or plane-stress plastic zones in polymer films was demonstrated [8, 9]. This method together with a new technique [9], which can be used to create a crack (typically $10\mu m$ wide, $100\mu m$ in length) in a polymer thin film, allows one to measure accurately the displacement profiles along the crazes or plastic zones extending from the tips of a crack in a polymer thin film in a homogeneous tensile stress field. Assuming linear elastic behaviour of the material outside these plastic zones, there must exist a unique stress field solution which corresponds to the measured displacement profiles of the plastic zones and the condition that the tensile stresses are zero across the crack. The aim of this paper is to obtain analytically the surface stress profile along the plastic zones at the tips of the crack for this mixed boundary value problem. The mathematical derivation described below makes no assumptions which are uniquely applicable only to polymeric materials. It can be used therefore in any material that satisfies all the conditions (narrow plastic zone, linear elastic behaviour outside the zone) of this analysis. The surface stresses derived in this paper are an exact solution for the stress field of the plastic zone. Therefore, instead of comparing the displacement with those of the Dugdale model, the displacements measured along the plastic zone can now be used directly to generate the surface stress profile which can be compared directly with the constant stress profile of the Dugdale model. Knowing both the displacements and stresses everywhere along the plastic zone, other micromechanical parameters, such as the plastic work for incremental crack advance, may be computed.

2. Theory

Let us consider a simple two-dimensional system of an infinite isotropic elastic sheet containing a crack described by the co-ordinates $|x| \leqslant c, y = 0$ and illustrated in Fig. 1a. A uniform tensile stress $\sigma_{yy} = \sigma_\infty$ is applied far from the crack which produces a Mode I displacement of the crack surfaces. To eliminate the stress singularity at the crack tips, the material along $y = 0$ ahead of the crack tip at $x = c$ is allowed to open as far as $x = a$, the opposing surfaces being attracted towards each other by cohesive stresses, which act in the region $c \leqslant x \leqslant a$ $(y = 0)$ also shown in Fig. 1a. This region is referred to hereafter as the plastic deformation zone; by virtue of symmetry, a similar plastic deformation zone is assumed to exist near the other crack tip. The cohesive stresses $\sigma_{yy}(x, y = 0)$ are represented by $S(x)$; and $w(x)$ is the y-component of the displacement of the surface of the upper half-block $y > 0$, $-w(x)$ being the corresponding displacement of the surface of the lower half-block $y < 0$. It is assumed that the material within the half-blocks of solid still obeys the constitutive equations of infinitesimal linear elasticity and the plastic deformation is confined to narrow wedge-shaped zones, which can be treated as linear extensions of the crack. However, there are no assumptions necessary about the length of the plastic zone or about the constitutive relations of the material inside the plastic zone. The latter is the major difference between this plastic zone model and Dugdale plastic zone model, which assumes that the surface stress is constant over the plastic zone in advance of the crack tip, i.e. the material inside the Dugdale plastic zone is assumed to be a rigid–perfectly plastic solid.

We wish to solve for the surface stress profile along the plastic zones under the condition that the displacements along these plastic zones are known. Mathematically, this means we must solve the biharmonic equations, i.e. $\nabla^2\nabla^2 u = 0$, $\nabla^2\nabla^2 w = 0$ (where u and w are the x and y components of the displacement vector) under the following mixed boundary conditions:

(a) the surface traction is zero along the crack,

(b) the displacement profiles along plastic zones are known. Since the anti-plane strain, Mode III, (Fig. 1b) version of this problem is easier to solve than the Mode I (Fig. 1a) problem and since it is straighforward to convert the solution of the Mode III problem to that of the Mode I problem by making the replacements $\sigma_{zy}(y = 0) \to \sigma_{yy}(y = 0) = S(x)$, $v \to w$ and $G \to E^*/2$ (where v is the z-displacement of the Mode III crack surface, G is the shear modulus, ν is Poissons ratio and E^* = Young's modulus,

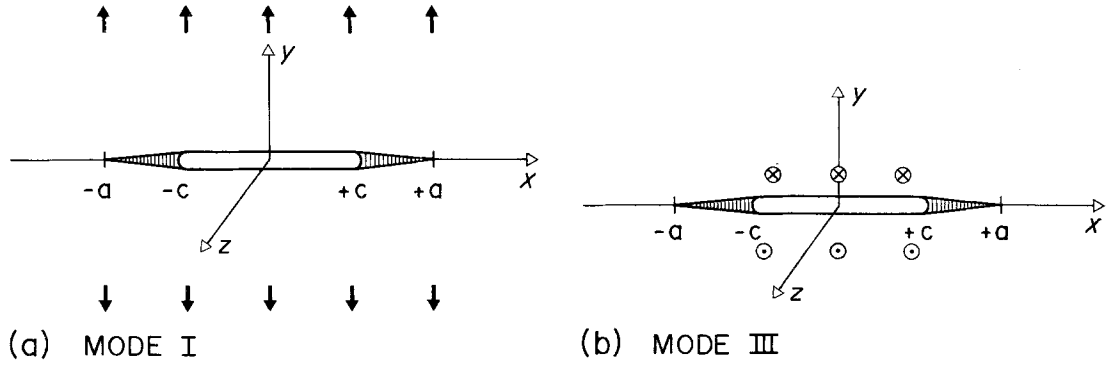

Figure 1 (a) Mode I and (b) Mode III crack and plastic zones.

E, for plane stress and $E^* = E/(1-\nu^2)$ for plane strain), this mixed boundary problem will be solved here first for the Mode III anti-plane strain case. As shown in Fig. 1b the Mode III anti-plane strain condition implies that $u = w = 0$ and $\partial v/\partial z = 0$. The only non-vanishing stress components are $\sigma_{zx} = G(\partial v/\partial x)$ and $\sigma_{zy} = G(\partial v/\partial y)$ and the equilibrium equations reduce to the single one $\nabla^2 v = 0$, which means that the displacement v must be a harmonic function.

In this paper, no attempt is made to solve directly for this harmonic function under the mixed boundary conditions; rather, this problem will be approached by using the results of dislocation theory. Dislocations can serve as basic elements in the macroscopic treatment of fracture because a crack or a plastic zone is equivalent to a continuous array of dislocations [20, 21]. However, it must be emphasized that the actual structure of the plastic zone is not necessarily that of a dislocation array. Rather, the elastic stresses in the region outside the zone (craze) are the same whether the surface displacement profile $v(x)$ is produced by an array of dislocations or by an array of any other structural element.

The plastic zones with known displacements are represented by continuous arrays of dislocations with the linear dislocations density $\alpha(x) = (-2/\mathbf{b})(\partial v(x)/\partial x)$ ("$\mathbf{b}$" is Burger's vector in dislocation theory; since we are using mathematical dislocations, $\mathbf{b}$ is set to be unity and will be omitted afterwards in all equations which follow*).

The two dimensional Mode III stress system can be represented conveniently by complex variables. In Fig. 1b, the stress at any point (x, y) is expressed as $\sigma(Z)$, where $Z = x + iy$ and $\sigma(Z) = \sigma_{xz}(Z) - i\sigma_{yz}(Z)$. The interest here is only on the surface stress profiles along or in front of the plastic zones on the x-axis; along this line $Z = x$. The crack is introduced in such a way that it modifies the initial stress field caused both by the applied tensile stress, σ_∞, and the dislocation arrays representing the plastic zones ahead of the crack tips.

First the stresses will be determined, assuming no crack exists. In this case the stress at a point x ($|x| \geqslant c$) will be composed of two parts: that due to the applied stress and that due to the stress $\sigma_\alpha(x)$ caused by the dislocation arrays representing the two plastic zones ahead of the crack tips. When the crack is introduced, the stress at this point will be modified by adding two induced stress components σ_∞^c and σ_α^c caused by the interaction between the crack and the two stress sources σ_∞ and $\sigma_\alpha(x)$ respectively. Thus, the stress $\sigma(x)$ at a point x will include four parts, i.e.

$$\sigma(x) = (\sigma_\infty + \sigma_\infty^c(x)) + (\sigma_\alpha(x) + \sigma_\alpha^c(x)). \quad (1)$$

The stress terms in the first parenthesis represent the stress at point x produced by the applied tensile stress acting on the crack in the absence of any plastic zones.

Representing the crack by a continuous array of dislocations, Bilby and Eshelby [20] obtained

$$\sigma_\infty + \sigma_\infty^c(x) = \frac{\sigma_\infty |x|}{i(x^2 - c^2)^{1/2}}. \quad (2)$$

The term $\sigma_\alpha(x)$ is the stress at point x due to the dislocation array of density $\alpha(x)$ and is given by

*While the magnitude of $\alpha(x)$ depends on the value chosen for $\mathbf{b}$, the expressions for the stress always contain a factor of $G\mathbf{b}$ multiplied by integrals of $\alpha(x)$. Hence the arbitrary choice of $\mathbf{b} = 1$ does not affect the stress field results while permitting simplification of the final equations.

$$\sigma_\alpha(x) = (G/2\pi i)\int_{PZ'} dx_1\alpha(x_1)\frac{1}{(x-x_1)}. \quad (3)$$

The integral here is over the region on the x-axis where dislocation density is not zero ($\alpha(x_1) \neq 0$), i.e. inside the two plastic zones (PZ). The last term, $\sigma_\alpha^c(x)$, is the stress caused by introducing a crack in the stress field of the dislocation arrays. This term can be expressed (for $|x| > c$) as [20]

$$\sigma_\alpha^c(x) = -(1/\pi)\int_{-c}^{+c} dx_1\sigma'_\alpha(x_1)\frac{(x_1^2-c^2)^{1/2}}{(x^2-c^2)^{1/2}} \times \frac{(\text{sgn}\,(x)) \times (\text{sgn}\,(x_1))}{(x-x_1)}. \quad (4)$$

Here sgn (x) means the sign of x and $\sigma'_\alpha(x_1)$ is the yz-component of the stress at point x_1 due to the dislocations pile-ups without the crack. The stress $\sigma'_\alpha(x_1)$ thus can be derived by taking only the yz-component part of Equation 3.

$$\sigma'_\alpha(x_1) = (G/2\pi)\int_{PZ} dx_2\alpha(x_2)\frac{1}{(x_1-x_2)}. \quad (5)$$

From the five equations above, the stress, $\sigma(x)$, at a point x can be obtained as a function of the dislocation density $\alpha(x)$, once a and c are determined. After substituting the term $\sigma'_\alpha(x_1)$ from Equation 5 into Equation 4 and changing the sequence of integration we find

$$\sigma_\alpha^c(x) = (G/2\pi)\int_{PZ} dx_1\alpha(x_1)\frac{\text{sgn}\,(x)I}{(x^2-c^2)^{1/2}}, \quad (6)$$

where

$$I = -(1/\pi)\int_{-c}^{+c} dx_2 \times \frac{\text{sgn}\,(x_2)(x_2^2-c^2)^{1/2}}{(x-x_2)(x_2-x_1)}. \quad (7)$$

Next the integral in Equation 7 is replaced by a contour integral, and this integral can be solved by complex variable integration methods outlined in the Appendix. The final result is

$$I = -i + i\left[\frac{\text{sgn}\,(x)(x^2-c^2)^{1/2}}{x-x_1} - \frac{\text{sgn}\,(x_1)(x_1^2-c^2)^{1/2}}{x-x_1}\right]. \quad (8)$$

Rearranging the terms in Equation 6 we obtain

$$\sigma_\alpha^c(x) = (G/2\pi i)\int_{PZ} dx_1\alpha(x_1) \times \frac{\text{sgn}\,(x)}{(x^2-c^2)^{1/2}} + (G/2\pi i)\int_{PZ} dx_1\alpha(x_1) \times \frac{(x_1^2-c^2)^{1/2}}{(x^2-c^2)^{1/2}} \times \frac{(\text{sgn}\,(x_1))(\text{sgn}\,(x))}{(x-x_1)} - (G/2\pi i)\int_{PZ} dx_1\alpha(x_1) \times \frac{1}{(x-x_1)}. \quad (9)$$

When $\sigma_\alpha^c(x)$ is substituted in Equation 1 for $\sigma(x)$, the last term (Equation 9) exactly cancels the $\sigma_\alpha(x)$ term (Equation 3). Therefore the stress at point x ($|x| \geqslant c$) produced by the plastic zones and crack without considering the applied stress is

$$\sigma_\alpha(x) + \sigma_\alpha^c(x) = (G/2\pi i)\int_{PZ} dx_1\alpha(x_1) \times \frac{(\text{sgn}\,(x))}{(x^2-c^2)^{1/2}} \times \left[1 + \frac{(\text{sgn}\,(x_1))(x_1^2-c^2)^{1/2}}{(x-x_1)}\right]. \quad (10)$$

To be useful, Equation 10 must be altered so that the singular part (which diverges when $|x| = c$) is separated from the non-singular part.

This separation is necessary because the stress singularity produced by the crack in the applied tensile stress field will be assumed to be cancelled out exactly by the stress singularity produced by the plastic zones (dislocation arrays) acting on the crack. This assumption, which is also the starting point of the Dugdale model, seems reasonable for static cracks and plastic zones. Since some stress singularity at the crack tip is necessary for a finite rate of crack advance, this assumption must be modified so that a small stress singularity is retained for the growing crack [22]. The relaxation of this assumption to provide for slow crack growth will not greatly affect the craze stress fields determined except very close to the crack tip.

The stress singularity caused by the applied stress and the crack is just the right hand side part of Equation 2. However, the separation of the singular part from the non-singular part in Equation 10 must be performed in such a way that no new singularity is introduced in the final form. That is, the stress singularity should occur only at the crack tips ($|x| = c$) but nowhere else in the final expression for the singular stress. This restriction provides a unique way to perform the mathematical separation. The result after the separation is

$$\sigma_\alpha(x) + \sigma_\alpha^c(x) = (G/2\pi i)\int_{PZ} dx_1\alpha(x_1)\,\text{sgn}\,(x)(x^2-c^2)^{1/2}$$

$$\times \left[\frac{\operatorname{sgn}(x_1)}{(x_1^2-c^2)^{-1/2}(x-x_1)} + \frac{1}{x_1^2-c^2} \right]$$

I II

$$+ (G/2\pi i)\int_{PZ} dx_1 \alpha(x_1) \frac{\operatorname{sgn}(x)}{(x^2-c^2)^{1/2}}$$

$$\times \left[\frac{\operatorname{sgn}(x_1)}{(x_1^2-c^2)^{1/2}}(-x-x_1) + \frac{x_1^2-x^2}{x_1^2-c^2} \right]. \quad (11)$$

III IV V

The first integral contains the non-singular part of the stress, while the second integral contains the singular part. Since the displacement profiles of the plastic zones are symmetric with respect to the origin, i.e. $v(x) = v(-x)$, the $\alpha(x)$ will be antisymmetric with respect to the origin ($\alpha(x) = -\alpha(-x)$). This property of $\alpha(x)$ makes the second(II), the fourth(IV), and the fifth(V) term in Equation 11 vanish. Therefore,

$$\sigma_\alpha(x) + \sigma_\alpha^c(x) = \frac{1}{i}\left[\frac{|x| I_1}{(x^2-c^2)^{1/2}} + \operatorname{sgn}(x)(x^2-c^2)^{1/2} I_2 \right], \quad (12)$$

where

$$I_1 = -(G/2\pi)\int_{PZ} dx \alpha(x) \frac{\operatorname{sgn}(x)}{(x^2-c^2)^{1/2}},$$

and

$$I_2 = (G/2\pi)\int_{PZ} dx_1 \alpha(x_1) \frac{\operatorname{sgn}(x_1)}{(x_1^2-c^2)^{1/2}(x-x_1)}.$$

The I_1 term represents the singular part of the stress while the I_2 term represents the non-singular part. By substituting the results of Equation 12 and Equation 2 into Equation 1 the total stress at a point x is obtained:

$$\sigma(x) = \frac{\sigma_\infty |x|}{i(x^2-c^2)^{1/2}} + \frac{I_1 |x|}{i(x^2-c^2)^{1/2}} + \frac{1}{i}(\operatorname{sgn}(x))(x^2-c^2)^{1/2} I_2. \quad (13)$$

The above equation actually contains two independent relations. Since the stress singularity at the crack tip must vanish, the first and second terms in Equation 13 should cancel each other. The positive stress singularity at crack tips caused by applied stress σ_∞ is eliminated by the negative stress singularity due to the plastic zones so that

$$\frac{\sigma_\infty |x|}{i(x^2-c^2)^{1/2}} + \frac{I_1 |x|}{i(x^2-c^2)^{1/2}} = 0. \quad (14a)$$

This relation expresses the applied stress σ_∞ in terms of dislocation density $\alpha(x)$.

$$\sigma_\infty = (G/2\pi)\int_{PZ} dx \alpha(x) \frac{\operatorname{sgn}(x)}{(x^2-c^2)^{1/2}}. \quad (14b)$$

After this cancellation the remaining equation gives $\sigma(x)$, the stress at point x outside the crack in terms of $\alpha(x)$, i.e.,

$$\sigma(x) = (G/2\pi i)\operatorname{sgn}(x)(x^2-c^2)^{1/2} \times \int_{PZ} dx_1 \alpha(x_1) \frac{\operatorname{sgn}(x_1)}{(x_1^2-c^2)^{1/2}(x-x_1)}. \quad (15)$$

The yz-component of this stress $\sigma(x)$ is

$$\sigma_{yz}(x) = (G/2\pi)\operatorname{sgn}(x)(x^2-c^2)^{1/2} \times \int_{PZ} dx_1 \alpha(x_1) \frac{\operatorname{sgn}(x_1)}{(x_1^2-c^2)^{1/2}(x-x_1)}. \quad (16)$$

These are the results for a Mode III crack; for a Mode I crack

$$\sigma_\infty = (\sigma_{yy})_\infty = \frac{E^*}{4\pi}\int_{PZ} dx \alpha(x) \frac{\operatorname{sgn}(x)}{(x^2-c^2)^{1/2}}, \quad (17)$$

and

$$S(x) = \sigma_{yy}(x; y=0) = \frac{E^*}{4\pi}\operatorname{sgn}(x)(x^2-c^2)^{1/2} \times \int_{PZ} \frac{dx_1 \alpha(x_1)}{(x_1^2-c^2)^{1/2}} \frac{\operatorname{sgn}(x_1)}{(x-x_1)} \quad (18)$$

where $\alpha(x_1) = -2(\partial w(x)/\partial x)$ and $w(x)$ is the surface displacement profile of the plastic zones.

Equations 14 and 15, or their equivalent Mode I expressions, which are the final results, will be examined for some limiting cases as follows: First, if the crack does not exist ($c \to 0$), Equation 15 will reduce to Equation 19 as follows

$$\sigma(x) = (G/2\pi i)\int_{PZ} dx_1 \alpha(x_1) \frac{x}{x_1(x-x_1)}$$

$$= (G/2\pi i)\int_{PZ} dx_1 \alpha(x_1) \times \left[\frac{\operatorname{sgn}(x_1)}{(x_1^2-c^2)^{1/2}} + \frac{1}{x-x_1} \right]$$

$$= (\sigma_\infty/i) + (G/2\pi i)\int_{PZ} dx_1 \alpha(x_1) \frac{1}{x-x_1}. \quad (19)$$

Equation 19 is the stress at point x with the plastic zones and applied stress but no crack.

Second, from Equation 16 at a point far away from the origin ($x \to \infty$)

$$\sigma(x) = (G/2\pi i)\int_{PZ} dx_1\alpha(x_1)\frac{\text{sgn}(x_1)}{(x_1^2-c^2)^{1/2}} \times \lim_{x\to\infty}\left[\frac{(x^2-c^2)^{1/2}\,\text{sgn}(x)}{x-x_1}\right]$$

$$= (G/2\pi i)\int_{PZ} dx_1\alpha(x_1)\frac{\text{sgn}(x_1)}{(x_1^2-c^2)^{1/2}}$$

$$= (\sigma_\infty)/i. \qquad (20)$$

This result shows that the stress is just the applied stress at points far away.

Third, for $|x| < c$, $(x^2-c^2)^{1/2}$ is imaginary and Equation 15 does not have an imaginary part. From the Equation $\sigma(x) = \sigma_{xz}(x) - i\sigma_{yz}(x)$ therefore $\sigma_{yz}(x) = 0$ when $|x| < c$. In the Mode I deformation case, this corresponds to $\sigma_{yy} = 0$ which is just the boundary condition that the surface traction is zero along the crack.

The formulation of the above derivation can also be specialized to the case of the semi-infinite crack which lies on the negative x-axis with its crack tip at $x = 0$ and a plastic zone that extends from $x = 0$ to $x = a$. Substituting $x \to x + c$, $x_1 \to x_1 + c$ and then letting c approach infinity in Equation 16 leads to the result

$$\sigma(x) = (G/2\pi i)\int_{PZ} dx_1\alpha(x_1)\frac{1}{x-x_1}(x/x_1)^{1/2}, \qquad (21a)$$

or for Mode I

$$S(x) = (E^*/4\pi)\int_{PZ} dx_1\alpha(x_1)\frac{1}{x-x_1}(x/x_1)^{1/2}. \qquad (21b)$$

Equation 21a is the result previously derived directly for the semi-infinite crack case by Hart [22].

For numerical calculations, Equations 14, 16, 17 and 18 can be further simplified to include only the integral along the positive x-axis by using the anti-symmetric properties of $\alpha(x)$. Equation 17 can be expressed as

$$\sigma_\infty = (E^*/2\pi)\int_c^a dx\alpha(x)\frac{1}{(x^2-c^2)^{1/2}}, \qquad (22)$$

and Equation 18 is reduced to

$$S(x) = (E^*/2\pi)x(x^2-c^2)^{1/2} \times \int_c^a \frac{dx_1\alpha(x_1)}{(x_1^2-c^2)^{1/2}}\frac{1}{x^2-x_1^2}. \qquad (23)$$

Here E^* should be replaced by $2G$ to find the Mode III equivalents.

These two equations are in closed form and can be used to obtain the applied stress and the stress profile outside the crack provided that the dislocation density profile is known. A computer program was developed to integrate numerically Equations 22 and 23. The input required for this program is the displacement profile ($w(x)$) along the plastic zone. Derivatives of this displacement profile are obtained by the subroutine SPLINE and SEVAL, and smoothed by hand. This dislocation density profile then serves as the input for the subroutine which determines σ_∞ and $S(x)$.

In this subroutine, the integral from c to a is first separated into several intervals such that the intervals are smaller where the gradient of $\alpha(x)$ is larger. Numerical integrations over these intervals are carried out using a Gaussian quadrature formula with 32 points.

To obtain $S(x)$, if the point x is inside the plastic zone, two points $x+\delta$, $x-\delta$ on either side of x are chosen, and the integration is then performed from c to $x-\delta$, and from $x+\delta$ to a separately. The value of δ will be decreased gradually until the sum of these two integrals reaches a constant value. In practice, δ is set to be $10^{-12}c$ although usually there is little change in the result when δ is smaller than $10^{-6}c$. The final output is the applied stress σ_∞ and the craze surface stress at point x ($S(x)$) as a function of x. The range of x extends from crack tip to beyond plastic zone tip.

3. Testing the stress analysis procedure

The stress analysis procedure has been tested by using the known analytical results of the Dugdale model [5]. In the Dugdale model the surface stress, S, along the plastic zone is a constant, σ_y. The condition that stress singularities must vanish leads to the following Dugdale model condition (which is equivalent to our Equation 17)

$$c/a = \cos(\sigma_\infty\pi/2\sigma_y). \qquad (24)$$

After three out of the four parameters, crack half length c, crack half length plus zone length a, σ_∞, and σ_y are fixed, the fourth one is determined by Equation 24. Moreover, once these parameters are known the entire displacement profiles for the plastic zones are determined.

It is convenient to define an angular variable $\beta = \arccos(x/a)$ and $\beta_c = \arccos(c/a) = (\sigma_\infty\pi/2\sigma_y)$.

The crack and zone surface displacement $w(\beta)$ is given by

$$w(\beta) = (a\sigma_y/\pi E^*)H(\beta, \beta_c), \quad (25)$$

where

$$H(\beta, \beta_c) = \cos(\beta) \ln\left[\frac{\sin^2(\beta_c - \beta)}{\sin^2(\beta_c + \beta)}\right] + \cos(\beta_c) \ln\left[\frac{(\sin(\beta_c) + \sin(\beta))^2}{(\sin(\beta_c) - \sin(\beta))^2}\right].$$

The dislocation density at a point x is

$$\alpha(\beta) = (-\sigma_y/\pi E^*) \ln\left[\frac{\sin^2(\beta_c - \beta)}{\sin^2(\beta_c + \beta)}\right]. \quad (26)$$

The stress is zero on the crack surface, a constant value σ_y along plastic zones, and decays gradually to the applied stress σ_∞ far away from origin.

In testing the computer program, c, a, σ_y are chosen to be 1.0 mm, 5.0 mm, and 3.0 MPa respectively (E^* is chosen to be 6.28 MPa). From Equation 25 the displacement profile $w(x)$ is obtained as a function of x. This displacement profile is used as the input of the computer program. The computed stress profile, displacement profile, and dislocation density profile for these conditions are shown in Figs 2, 3, and 4 respectively. The surface stress profile closely mirrors the behaviour expected from the Dugdale model, with the stress over the plastic zone being very near the correct value of $\sigma_y = 3$ MPa. The computed applied stress σ_∞ is 2.6119 MPa, which is in excellent agreement with the value 2.6155 MPa calculated from Equation 24.

In testing the distributed dislocation analysis with the Dugdale model it was observed that the results are quite sensitive to the integration of $\alpha(x)$ at the crack tip. As a result of the step change in stress at the crack tips, there is a local logarithmic singularity there in $\alpha(x)$, as can be seen from Equation 26. When values of $\alpha(x)$ are determined from experiment however, $\alpha(x)$ will not be singular at the crack tips because $\alpha(x)$ must be found from the difference between $w(x)$ from points along the zone spaced at least 0.5 μm apart. The absence of the singularity in the experimental $\alpha(x)$ means that the $S(x)$ computed from these data will not fall abruptly at the crack tips; in addition small errors (of the order of 10%) are introduced into σ_∞.

To correct for this experimental limitation, Equation 26 is used to reintroduce a singularity in $\alpha(x)$ at the crack tip. The dislocation density $\alpha(x_t)$ is determined at a point x_t (corresponding to β_t) close to the crack tips. In the region closer to the crack tip (between β_t and β_c), $\alpha(\beta)$ is computed from

$$\alpha(\beta) = \alpha(\beta_t) \ln\left[\frac{\sin^2(\beta_c - \beta)}{\sin^2(\beta_c + \beta)}\right] \Big/ \ln\left[\frac{\sin^2(\beta_c - \beta_t)}{\sin^2(\beta_c + \beta_t)}\right]. \quad (27)$$

The use of Equation 27 to extrapolate $\alpha(x)$ to the crack tip results in an abrupt fall in $S(x)$ at the crack tip and correct values of σ_∞.

4. Experimental procedure

An experimental method to find the displacement profile along the plastic zone in polymers has been developed by Lauterwasser and Kramer [8]. They bonded thin films of polystyrene, which were cast from solution, to annealed copper grids. Putting these copper grids under tension, crazes were grown from dust particles. Recently, Donald and Kramer [9] used the intense electron beam of a JEOL 733 Superprobe to "burn" a crack into

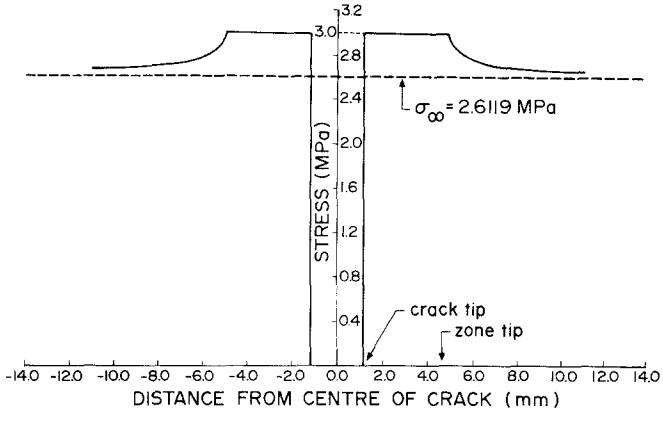

Figure 2 Surface stress profiles of the Dugdale model.

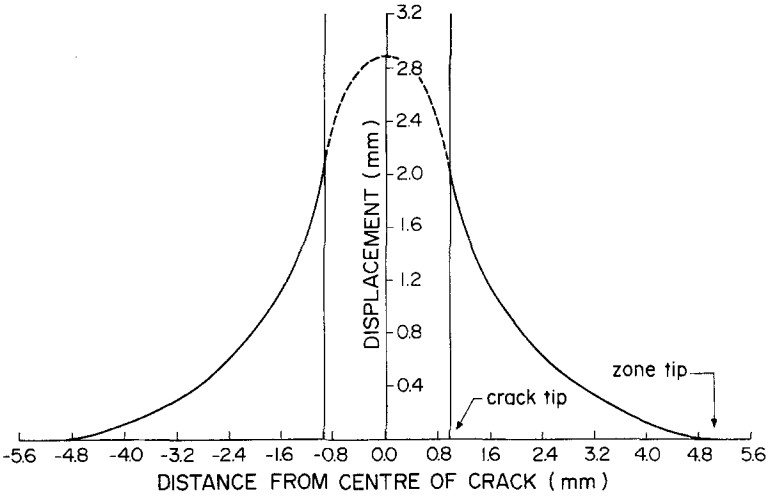

Figure 3 Displacement profile of the Dugdale model.

thin films of polycarbonate (PC), polystyrene (PS), and other polymers. Crazes or deformation zones may be grown from the tips of these cracks.

To demonstrate the stress analysis procedure it will be applied both to a craze in a PS film grown from a "crack" created with the electron microprobe and to a deformation zone in PC previously grown and analysed by Donald and Kramer [9].

The displacement profiles along the crazes are obtained directly from the quantitative analysis of the TEM plates by a method developed by Lauterwasser and Kramer [8]. By using the relation

$$w(x) = \tfrac{1}{2}T(x)(1 - v_f(x)) \qquad (28)$$

they obtain the craze surface displacement at point x, $(w(x))$ from the craze thickness $(T(x))$ and volume fraction of polymer fibrils $(v_f(x))$ at point x. The craze thickness profile is measured directly from the electron micrograph sequences along the craze. The local volume fraction of polymer material in the craze is determined from the microdensitometer measurements of the optical densities (on the electron image plate) of the craze $(\phi_c(x))$, the film (ϕ_f) and a hole in the film (ϕ_h) by using the equation

$$v_f(x) = 1 - \frac{\ln(\phi_c(x)/\phi_f)}{\ln(\phi_h/\phi_f)} \qquad (29)$$

The films of PC, which were 0.85 μm thick, were annealed below T_g and then strained. Opti-

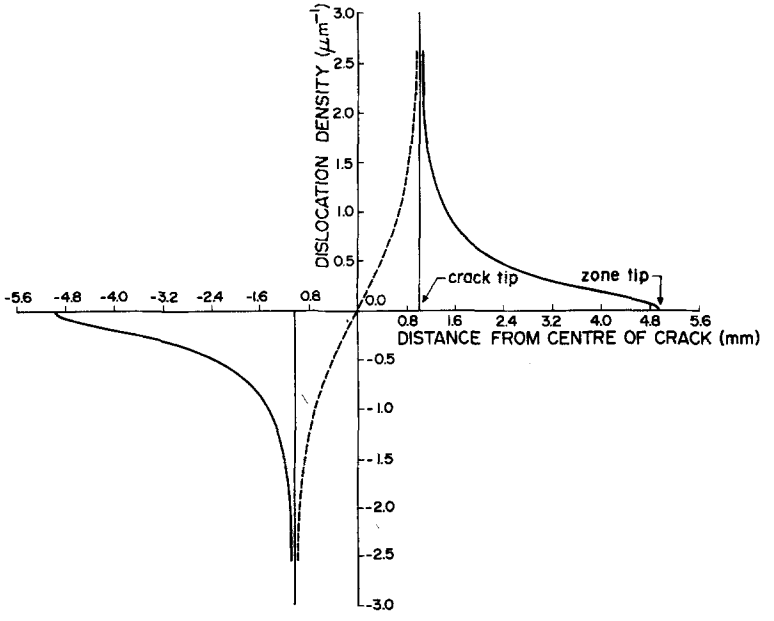

Figure 4 Dislocation density profile of the Dugdale model (Burger's vector "**b**" is set to be 1 μm).

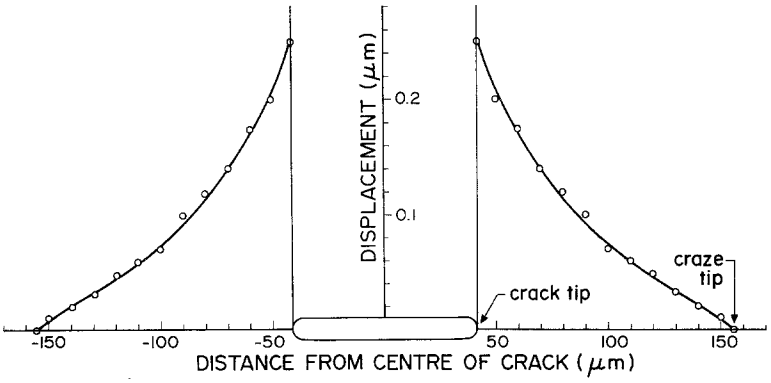

Figure 5 Displacement profile of air craze of PS.

cal micrographs of the plane stress deformation zones which grow from the crack tip in the PC film were taken through a conventional optical microscope. Unlike crazes, these zones contain an unfibrillated web of drawn polymer material. To obtain the displacement profile, $w(x)$, the measurements of these optical microscope pictures were combined with TEM measurements of thickness fraction (v_f) obtained in the same manner as Lauterwasser and Kramer did in their polystyrene experiment.

5. Results and discussion

Precracked films of PS, 0.75 μm thick, were strained to produce crazes at the crack tips. TEM micrographs of an air craze in a PS film are taken and analysed. The displacement profile is shown in Fig. 5 and the dislocation density profile is shown in Fig. 6. The surface stress profile of the craze in the PS film is obtained from the distributed dislocation analysis and shown in Fig. 7. This stress profile exhibits the same characteristics (a maximum at the crack tip falling to a nearly constant value along the craze) as the surface stress profile previously obtained by Chan, Donald and Kramer [23] on different crazes in PS. They made indentation marks in the PS film to serve as cracks and initiated crazes from these cracks. The Fourier transform procedure due to Sneddon [24] was used to compute the surface stress profile from the equations

$$S(x) = \Delta S(x) + \sigma_\infty \tag{30}$$

$$\Delta S(x) = -\frac{2}{\pi}\int_0^\infty d\xi \bar{p}(\xi)\cos(x\xi), \tag{31}$$

where

$$\bar{p}(\xi) = (\xi E^*/2)\int_0^a dx w(x)\cos(x\xi). \tag{32}$$

This method requires that the displacements along the crack be known, as well as those along the craze deformation zone. While using the same TEM quantitative analysis to obtain the displace-

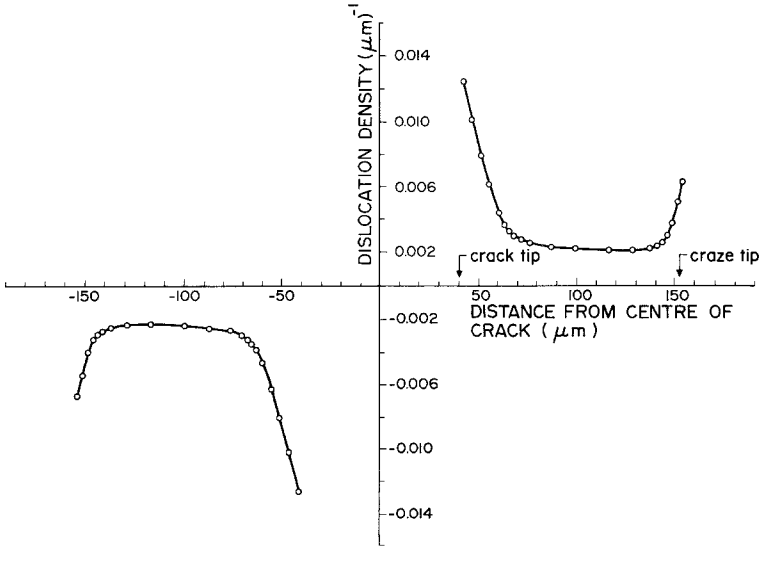

Figure 6 Dislocation density of air craze of PS (Burger's vector "**b**" is set to be 1 μm).

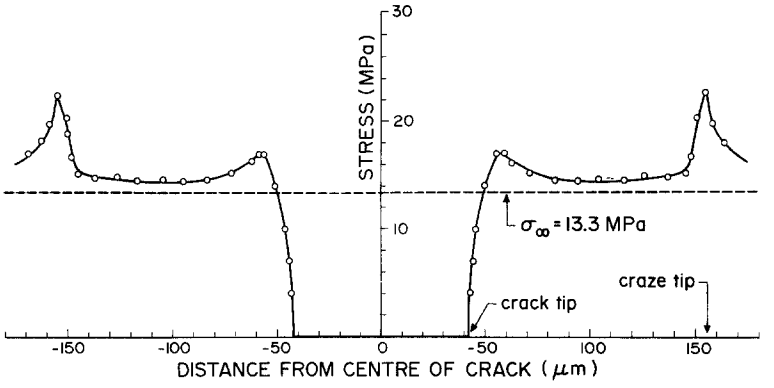

Figure 7 Surface stress profile of air craze of PS.

ment profile along the craze, they estimated the crack surface displacements from those of the Dugdale model and joined these displacements smoothly with the displacements measured in the region of the craze.

The displacement profile of the plastic deformation zone in PC, 40 sec into its growth, is used in the distributed dislocation analysis as described above. The surface stress profile obtained in this way is shown in Fig. 8. The applied stress, σ_∞, computed from Equation 22 is 33.9 MPa. In the stress analysis of Donald and Kramer [9] of the deformation zone in PC, the measured $w(x)$ profile along the deformation zone and the Fourier transform method were used to calculate the surface stress profile. By measuring the displacement w_0 in the centre of the crack by optical microscopy together with the values of c and a, they calculated the crack displacements from the Dugdale model and smoothly joined this displacement profile to the displacements measured in the deformation zone (Fig. 9). The surface stress profile obtained in this method is shown in Fig. 10, and the applied stress, σ_∞, calculated from Dugdale model from the measured w_0 is 37.4 MPa.

The surface stress profile computed by either method exhibits the same characteristics. Along most of the zone the stress is approximately constant while there is a stress concentration at the zone tip. The difference in the values of the applied stress calculated by the different methods is 3.5 MPa which is less than 10% of σ_∞. The difference in the stress at the zone tips is larger, 112 MPa as opposed to 87 MPa, a difference of about 25%. However, from Equation 23 the local stress $\sigma(x)$ is proportional to

$$\int \mathrm{d}x_1 \frac{\alpha(x_1)}{(x_1^2 - c^2)^{1/2}} \frac{1}{x^2 - x_1^2}$$

and is thus strongly dependent on the local value

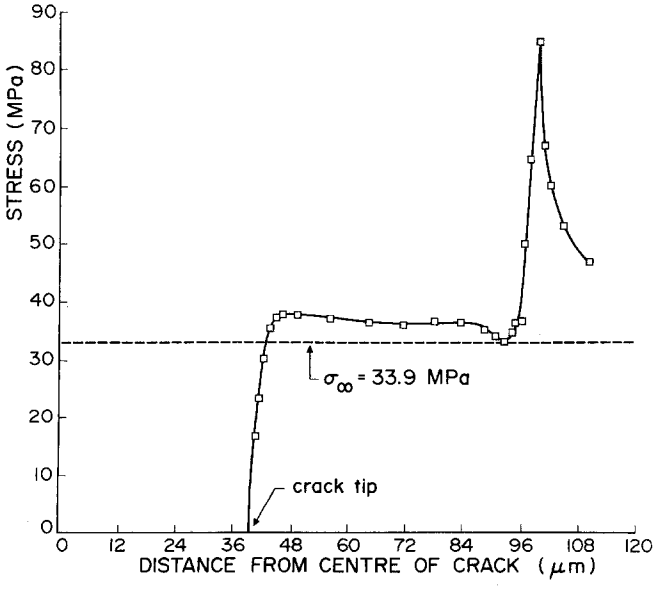

Figure 8 Surface stress profile of plastic deformation zone of PC calculated by distributed dislocation method.

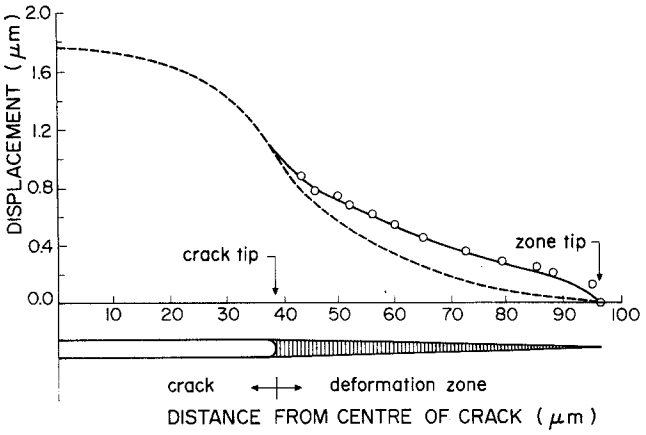

Figure 9 Experimental measured displacement profile (-o-) and Dugdale model displacement profile (---) of plastic deformation zone of PS, reproduced by permission from Donald and Kramer [9].

of the displacement gradient because of the factor $(x^2 - x_1^2)^{-1}$. At the zone tip there is a sharp drop in the displacement (i.e., a sudden increase in $\alpha(x)$), and this sharp drop is reflected in the stress concentration. It is obvious that a slight change in the input displacement profile near zone tip region can generate a large variance in the magnitude of stress concentration. Considering that the displacement curve was digitized separately for the tests of the two methods, the difference in the stress at the zone tip is understandable.

Although both the above methods can be used to obtain the surface stress profile and give approximately the same result for the plane stress plastic zone, there is a fundamental difference between them. Equation 22 and Equation 23 are exact solutions for the mixed boundary value problem; the error in the final result of the stress profile is introduced entirely from the experimental limitations in determining the displacement profile. The only data required in this method are the displacements along the deformation zones; moreover, there is no restriction on this displacement profile i.e., it need not necessarily resemble that of the Dugdale model.

On the other hand, the joining of crack displacements calculated from the Dugdale model to that of the deformation zone obtained from experiment gives a satisfactory solution of the stress profile since the local stress at a point on deformation zone is determined largely by the local displacement gradient and is not very sensitive to the approximate Dugdale displacements in the crack region. The other reason for this satisfactory result is due to the fact that the difference between the displacement profile of the deformation zone measured by experiment and the Dugdale displacement profile calculated from the three measured parameters (c, a, and w_0) is not very large, as shown in Fig. 9. The applied stress σ_∞, which in the approximate method is calculated from the experimental measured crack centre displacement (w_0) using the Dugdale model, while also not exact, is close to the actual value.

The distributed dislocation method has the disadvantage of requiring rather accurate measure-

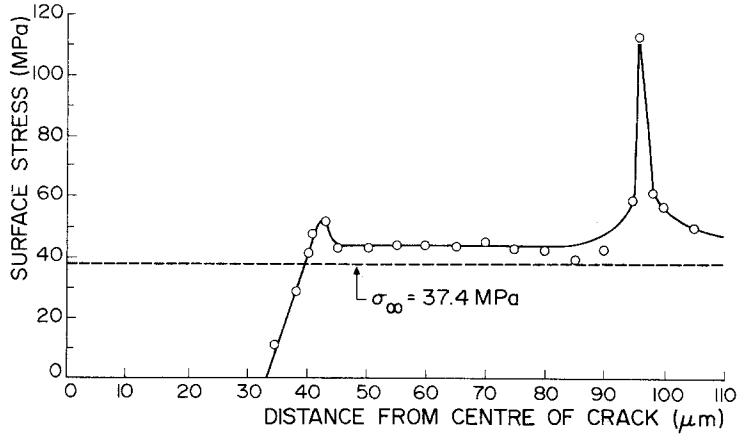

Figure 10 Surface stress profile of plastic deformation zone of PC calculated by Fourier transform method, reproduced by permission from Donald and Kramer [9].

ments of $w(x)$ at the crack tip. Both Equations 22 and 23 contain the factor $(x_1^2 - c^2)^{-1/2}$; hence the displacement gradient near the crack tip has a relatively large influence on both the values of σ_∞ and $\sigma(x)$. Consequently, the measurements of the displacements near the crack tip must be of high precision.

There are also limitations imposed by the assumptions necessary in developing the distributed dislocation method. The fact that the dislocation array in the derivation is limited to the x-axis requires that the plastic deformation of material be confined within a narrow wedge-shaped zone ahead of crack tip. Fortunately, many cases of plastic deformation in polymeric systems, such as crazes [6, 8, 17] in polystyrene and PMMA and deformation zones in polycarbonate [9] and poly-(2,6-dimethyl-1,4-phenylene oxide) (PPO) [25] have this narrow wedge-shaped zone characteristic.

The next important assumption is that the displacement profile is symmetric about $x = 0$, i.e. $w(x) = w(-x)$. This assumption means that $\alpha(x)$ will be antisymmetric and is essential in simplifying Equation 11 as well as in deriving Equations 19 and 20. In practice, this symmetry requirement is very difficult, though possible, to achieve. (The CO_2 crazes grown from cracks, introduced into polystyrene films by an electron microprobe beam, can satisfy this requirement.) The fact that the approximate Dugdale method, although replacing real displacements along the crack by the Dugdale displacements, can generate satisfactory results indicates that the plastic zone at one side of a long crack should bear negligible influence on the plastic zone at the other side of the crack. It is expected, therefore, that in the unsymmetric case the surface stress profile along each of the plastic zones can still be obtained through this method by measuring the displacement profile along each plastic zone and assuming symmetric conditions.

Finally, the distributed dislocation method can only be applied to the cases where the displacement or displacement gradient can be obtained from experiment. For crazes or deformation zones in polymers, this requirement can be achieved by quantitative transmission electron microscopy or combined TEM and optical microscopy. Combining these experimental procedures with the theoretical stress field analysis, studies of the micromechanics deformation zones and crazes in glassy polymer can be performed. In most previous applications of the TEM methods, the absolute values of $S(x) = \Delta S(x) + \sigma_\infty$ were considerably less certain than the craze or zone self-stress $\Delta S(x)$. An estimate of σ_∞ was made by assuming $\sigma_\infty = \epsilon E$ where ϵ is the strain applied to the grid. No way of correcting for either slack in the film or residual biaxial stress resulting from the bonding operations was possible. Using the distributed dislocation method to analyse TEM measurements of $w(x)$ of crazes or deformation zones grown from crack tips, it is now possible to determine both $\Delta S(x)$ and σ_∞ to the same degree of accuracy.

Acknowledgements

The financial support of this work by the U.S. Army Research Office, Durham, is gratefully acknowledged. The research also benefitted greatly from the use of the facilities of the Cornell Materials Science Center which is funded by the National Science Foundation. We would like to thank Professor E. W. Hart for stimulating discussion on the distributed dislocation stress analysis. We also thank Dr. A. M. Donald for permitting us to use some of her experimental results.

Appendix: Complex variable integration

The purpose of this Appendix is to compute the integral I, where

$$I = -(1/\pi)\int_{-c}^{+c} dx_2 \frac{\text{sgn}\,(x_2)(x_2^2 - c^2)^{1/2}}{(x - x_2)(x_2 - x_1)}$$

$$= -(1/\pi)\int_{-c}^{+c} dx_2 G. \qquad \text{(A1)}$$

This integral is integrated along the x-axis, therefore, x, x_1, x_2 can be replaced by complex variables z, z_1, z_2 respectively and the integration is carried out on the real axis of the complex plane. The line integral of G ($\int_{-c}^{+c} dz_2 G$) is replaced by a contour integral ($\oint_{c_0} dz_2 G$) (Fig. A1). Then the integral loop c_0 is expanded to an infinite radius loop in such a way that the singular points at z and z_1 are excluded (Fig. A2). Since G is analytic everywhere except at z and z_1, there is no change in the value of integral during the expansion process. The integral I than equals to the sum of three integrals, i.e.,

$$I = -(1/\pi)\int_{-c}^{+c} dz_2 G$$

$$= -(1/2\pi)\oint_{c_0} dz_2 G$$

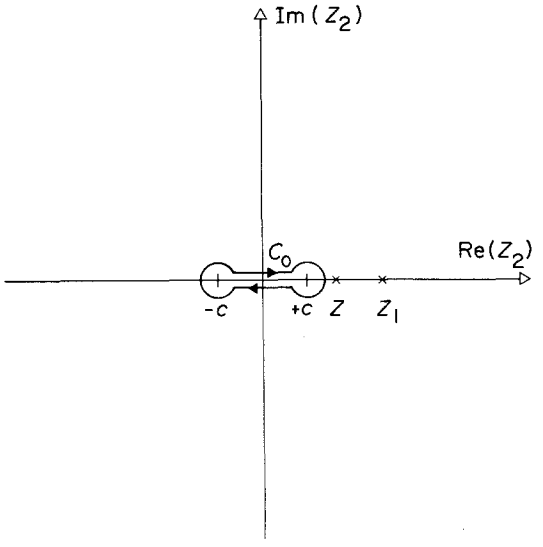

Figure A1 Contour integral C_0.

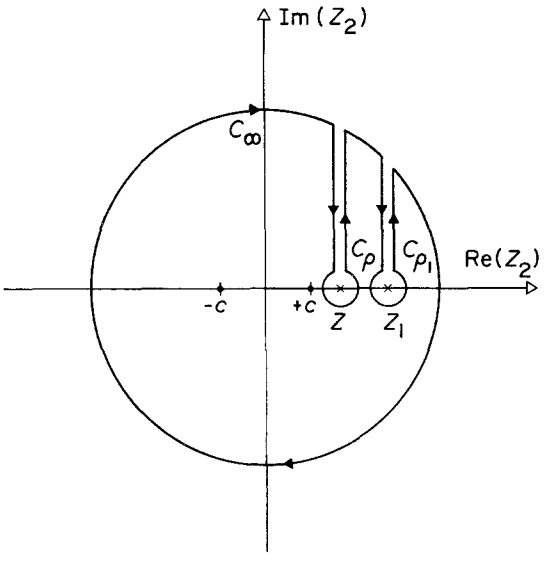

Figure A2 Contour integral C_∞, C_ρ and C_{ρ_1}.

$$= -(1/2\pi)\cdot\left(\oint_{C_\infty} + \oint_{\rho} + \oint_{\rho_1}\right) dz_2 G \quad \text{(A2)}$$

To evaluate $\oint_{C_\infty} dz_2 G$, the following substitutions are made: $z_2 \to re^{i\theta}$, $dz_2 \to ire^{i\theta}\,d\theta$ (the "dr" term vanishes since the circular integral $\oint_{C_\infty}$ is taken along a constant radius). Then let r approach infinity and we have:

$$\oint_{C_\infty} dz_2 G = \lim_{r\to\infty} \int_{2\pi}^{0} dz_2 \frac{(z_2^2 - c^2)^{1/2}}{(z - z_2)(z_2 - z_1)}$$

$$= \int_{2\pi}^{0} ire^{i\theta}\,d\theta \frac{1}{-re^{i\theta}}$$

$$= 2\pi i. \quad \text{(A3)}$$

To evaluate $(\oint_\rho + \oint_{\rho_1})dz_2 G$, G is separated into two terms:

$$G = \frac{(z_2^2 - c^2)^{1/2}}{(z - z_2)(z_2 - z_1)}$$

$$= \frac{(z_2^2 - c^2)^{1/2}}{z_1 - z}\left(\frac{1}{z_2 - z} - \frac{1}{z_2 - z_1}\right). \quad \text{(A4)}$$

According to the residue theorem, the contour integrals around the singularity at $(z_1 - z)^{-1}$ are

$$\left(\oint_\rho + \oint_{\rho_1}\right) dz_2 G = 2\pi i(K_1 - K_2) \quad \text{(A5)}$$

where K_1 and K_2 denote the residues of G at z and z_1

$$K_1 = \frac{(z^2 - c^2)^{1/2}}{z_1 - z} \quad \text{(A6)}$$

$$K_2 = \frac{(z_1^2 - c^2)^{1/2}}{z_1 - z}. \quad \text{(A7)}$$

After inserting Equations A3 and A5 into A2 we have

$$I = -(1/2\pi)\left\{2\pi i + 2\pi i \times \left[\frac{(z^2 - c^2)^{1/2}}{z_1 - z} - \frac{(z_1^2 - c^2)^{1/2}}{z_1 - z}\right]\right\}. \quad \text{(A8)}$$

Since the integral we wish is confined to the x-axis, z and z_1 are changed back to x and x_1 and finally we have

$$I = -i + i\left[\frac{\text{sgn}\,(x)(x^2 - c^2)^{1/2}}{x - x_1} - \frac{\text{sgn}\,(x_1)(x_1^2 - c^2)^{1/2}}{x - x_1}\right] \quad \text{(A9)}$$

References

1. F. A. McCLINTOCK and G. R. IRWIN, "Fracture Toughness Testing", ASTM STP 381, (1965) 84.
2. G. T. HAHN, M. F. KANNINEN and A. R. ROSENFIELD, *Ann. Revs. Mater. Sci.* **2** (1972) 381.
3. L. N. MAREAL, P. V. OSTERGREN and W. J. RICE, Jr., *Int. J. Fact. Mech.* **7** (1971) 143.
4. G. T. HAHN and A. R. ROSENFIELD, *Acta Metall.* **13** (1965) 293.
5. D. S. DUGDALE, *J. Mech. Phys. Solids* **8** (1960) 100.
6. H. R. BROWN and I. M. WARD, *Polymer* **14** (1973) 469.
7. R. FERGUSON, G. P. MARSHALL and J. G. WILLIAMS, *ibid.* **14** (1973) 451.

8. B. D. LAUTERWASSER and E. J. KRAMER, *Phil. Mag.* **A39** (1979) 469.
9. A. M. DONALD and E. J. KRAMER, *J. Mater. Sci.* in press.
10. G. I. BARENBLATT, *J. Appl. Math.* **23** (1959) 622.
11. B. A. BILBY, A. H. COTTRELL and K. H. SWINDEN, *Proc. Roy. Soc.* **A272** (1963) 304.
12. J. N. GOODIER and F. A. FIELD, Proceedings of the International Conference on Fracture of Solids, edited by D. C. Drucker and J. J. Gilman, Met. Soc. Conferences, Vol. 20, (Interscience Publishers, New York, 1963) p. 103.
13. A. C. KNIGHT, *J. Polymer Sci.* **A3** (1965) 1845.
14. N. VERHEULPEN-HEYMANS and J. C. BAUWENS, *J. Mater. Sci.* **11** (1976) 7.
15. A. P. WILCZYNSKI, C. H. LIU and C. C. HSIAO, *Appl. Phys.* **48** (1977) 1149.
16. N. J. MILLS, *J. Mater. Sci.* **16** (1981) 1317.
17. G. P. MORGAN and I. M. WARD, *Polymer* **18** (1977) 87.
18. M. J. DOYLE and J. G. WAGNER, in Proceedings of the ACS Symposium on Toughness and Brittleness of Plastics, Sept. 1974, edited by R. D. Denim and A. D. Crugnola, Advances in Chemistry series 154 (American Chemical Society) p. 63.
19. S. T. ISRAEL, E. L. THOMAS and W. W. GERBERICH, *J. Mater. Sci.* **14** (1979) 2128.
20. B. A. BILBY and J. D. ESHELBY, in "Fracture", Vol. 1, edited by H. Liebowitz (Academic Press, NY, 1972) Chap. II, p. 111.
21. J. D. ESHELBY, in "Fracture Toughness", ISI Publication 121 (The Iron and Steel Institute, London, 1968) Chap. II, p. 55.
22. E. W. HART, Private Communication (1980).
23. T. CHAN, A. W. DONALD and E. J. KRAMER, *J. Mater. Sci.* **16** (1981) 679.
24. I. N. SNEDDON, "Fourier Transforms", (McGraw-Hill, New York, 1951) pp. 395–430.
25. A. M. DONALD and E. J. KRAMER, *J. Polymer Sci., Polymer Phys.* in press.

Received 8 October
and accepted 2 December 1981